Synthesis, Characterization, Antitubercular Activity, and Molecular Docking Studies of Pyrazolylpyrazoline-Clubbed Triazole and Tetrazole Hybrids

Mayursinh Zala,* Jwalant J. Vora, and Vijay M. Khedkar

Read Online

ACCESS | 📊 Metrics & More | 📖 Article Recommendations | SI Supporting Information

ABSTRACT: To increase the antitubercular potency, we synthesized a series of novel pyrazolylpyrazoline derivatives (**9a−p**) using the one-pot multicomponent reaction of the substituted heteroaryl aldehyde (**3a,b**), 2-acetyl pyrrole/thiazole (**4a,b**), and substituted hydrazine hydrates (**5−8**) in the presence of base NaOH as a catalyst in ethanol as the solvent at room temperature. Substituted heteroaryl aldehyde (**3a,b**) was synthesized from 5-chloro-3-methyl-1-phenyl-1*H*-pyrazole-4-methyl-carbaldehyde on protection with ethylene glycol followed by treatment with 4-amino triazole/5-amino tetrazole and then deprotection using acid. The salient features of the green protocol are the one-pot reaction, shorter reaction time, and straightforward workup procedure. All of the compounds were tested against *Mycobacterium tuberculosis* H_{37}Rv, wherein compounds **9i, 9k, 9l, 9o,** and **9p** were found to be most effective. The structures of newly synthesized compounds were determined using spectral methods. Furthermore, molecular docking investigations into the active site of mycobacterial InhA yielded well-clustered solutions for these compounds' binding modalities producing a binding affinity in the range from −8.884 to −7.113. Theoretical results were in good accord with the observed experimental values. The docking score of the most active compound **9o** was found to be −8.884, and the Glide energy was −61.144 kcal/mol. and it was found to accommodate well into the active site of InhA, engaging in a network of bonded and nonbonded interactions.
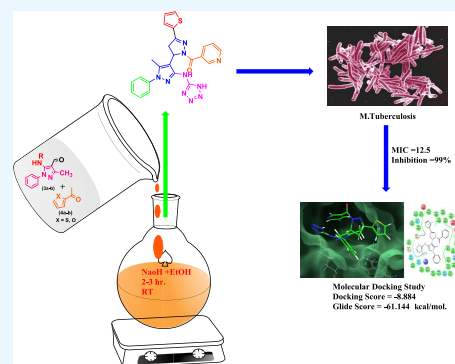
INTRODUCTION

In the recent past, according to the World Health Organization, 10 million new cases of tuberculosis were reported worldwide with 5.6 million men, 3.3 million women, and 1.1 million children.[1] Tuberculosis is the 13th leading cause of death and the second leading infectious killer after COVID-19. Tuberculosis predominantly triggered by *Mycobacterium tuberculosis* is one of the leading causes of human morbidity and mortality universally. Rifampicin, isoniazid, and ethambutol are the most effective drugs against tuberculosis that are available in the market, but bacteria have started developing resistance to these drugs, and it is a major public health concern in many countries for a couple of years. Nearly 6% of patients with tuberculosis have multidrug-resistant tuberculosis in the world, but in some areas, like Ukraine, Moldova, Kazakhstan, and Kyrgyzstan, this ratio increases up to 25%. Treatment for patients with multidrug-resistant tuberculosis is long, and patients with multidrug-resistant tuberculosis have less favorable outcomes than those treated for drug-susceptible tuberculosis.[2] The increasing occurrence of extensively drug-resistant (XDR)-TB coinfection with HIV and multidrug-resistant (MDR)-TB has driven the new tubercular drug discovery. Therefore it is an urgent need to develop antitubercular agents with a novel mechanism of action and potent biological activity against the drug-resistant tuberculosis strain.

In recent years, there has been endless interest in the exploration of novel pyrazole-clubbed pyrazoline moieties. A variety of modifications have been made to the pyrazole and pyrazoline moiety to boost its pharmacological effect because pyrazole−pyrazoline derivatives are widely studied for broad-spectrum biological activities.[3−12] The pyrazoline derivatives are widely used as anticancer,[13] antibacterial, antifungal,[14] antitubercular,[15] antimalarial,[16] anti-inflammatory,[17] etc. The chemistry of triazole- and tetrazole-fused heterocyclic derivatives has gathered a lot of attention in recent years due to their synthetic and biological importance. 1,2,4-Triazoles and their fused heterocyclic derivatives have been reported to possess a wide range of bioactivities such as neuroprotectant,[18] antioxidant,[19] antimalarial,[20] antileishmanial,[21] antiurease,[22] anticonvulsant,[23] and antiviral.[24] Tetrazole is a carboxylic acid bioisostere that can be used to substitute the carboxyl
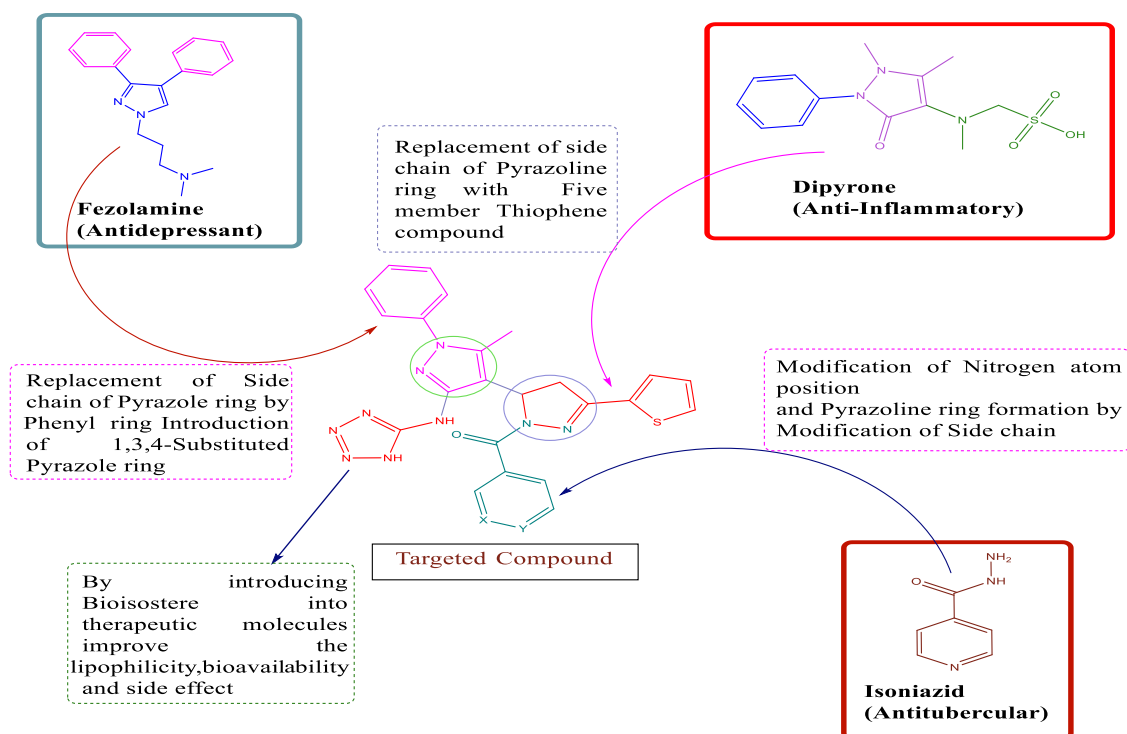
Figure 1. Design concept based on commercially available drugs comprising the heterocycles pyrazole and pyrazoline.

Scheme 1. Synthesis of Triazole/Tetrazole Hybrid Pyrazole Derivatives (3a,b)
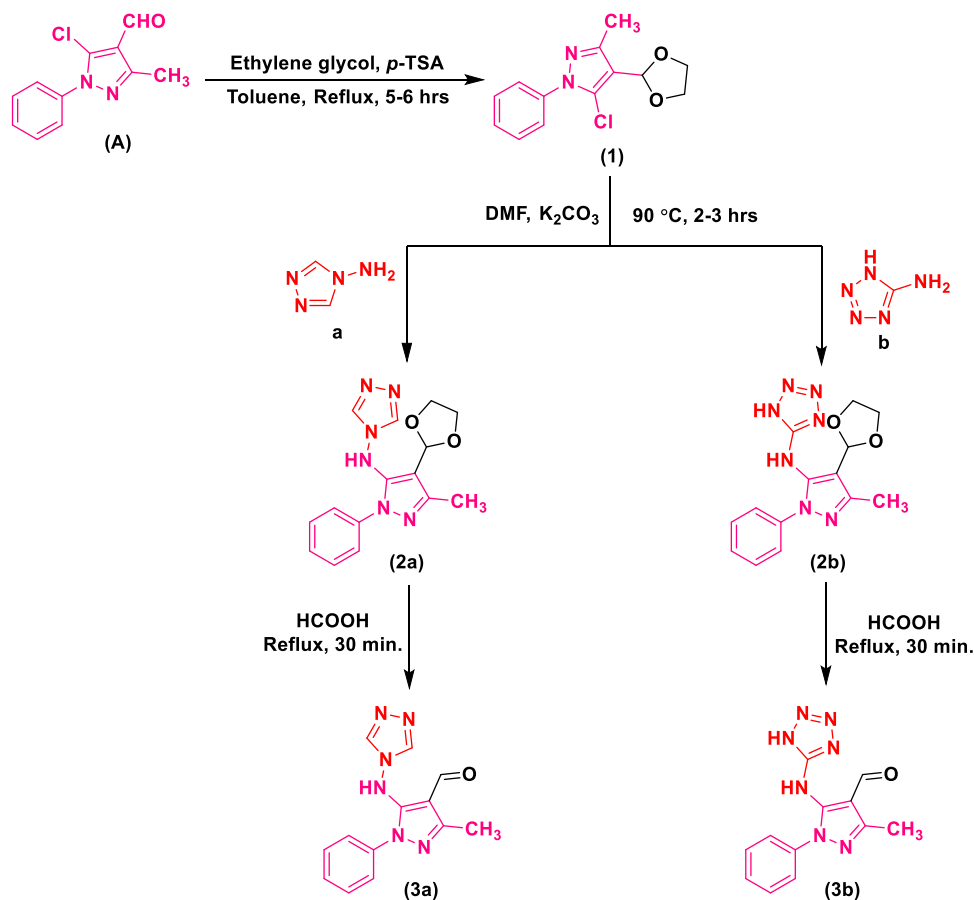
group in therapeutic molecules to improve lipophilicity, bioavailability, and side effects. Tetrazole can interact non-

covalently with a variety of enzymes and receptors in organisms, resulting in anticancer,[25] antifungal,[26] antitubercu-

Scheme 2. Synthesis of Novel Pyrazolylpyrazoline-Clubbed Triazole and Tetrazole Derivatives (9a−p)
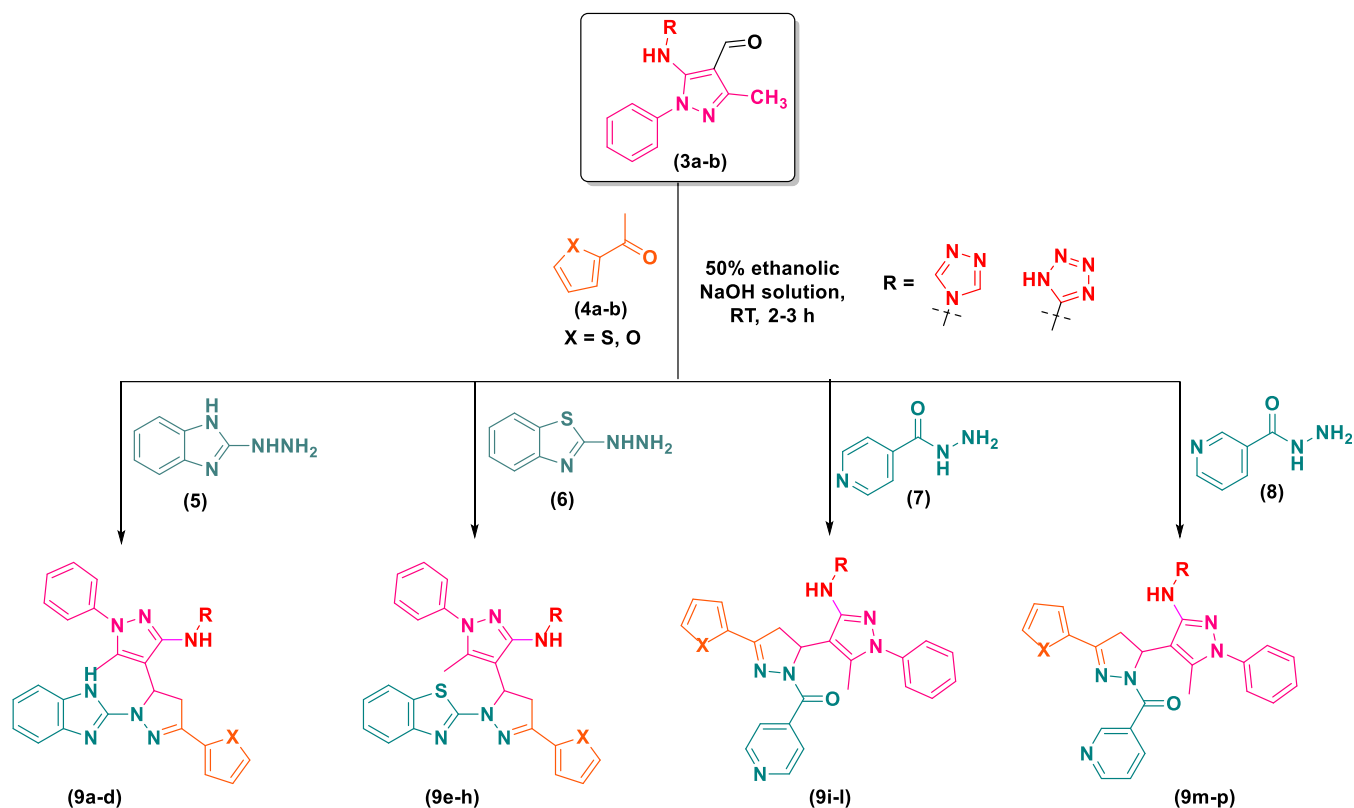
lar, and antimalarial[27] effects. Figure 1 illustrates commercially available pharmaceuticals active ingratiates with pyrazole and pyrazoline analogues. To improve antitubercular activity, our research work focused on the synthesis of certain novel structural hybrids of pyrazole−pyrazoline clubbed with triazole and tetrazole pharmacophores in a single molecular framework. Well-constructed innovative antitubercular drugs can illustrate two or more active skeletons to create a single molecule with improved biological potency in the hybrid approach to assimilate physiologically active heterocycles. The novel pyrazole- and pyrazoline-clubbed triazole and tetrazole hybrids described in this research work could be a valuable accumulation for the development of new antitubercular analogues with a novel mechanism of action. We synthesized scaffolds (9a−p) by incorporating the pharmacophores feature of isoniazid (antitubercular), fezolamine (antidepressant), and dipyrone (anti-inflammatory) in quest of novel heterocycles with good potency against drug-resistant tuberculosis. The structure−activity relationship (SAR) of the various pharmacophores was taken into account when designing the targeted compounds (9a−p; Figure 1). By altering the nitrogen atom and cyclization reaction of the side chain of the isoniazid drug, modification of the side chain of the dipyrone drug by adding the five-member heterocycles, and introducing the 1,3,4 substituents into the fezolamine drug, novel scaffolds (9a−p) were created and investigated for the in vitro antitubercular activity.

1-(2-(1H-Indol-3-yl)-5-(pyridin-4-yl)-1,3,4-oxadiazol-3(2H)-yl)-3-(2-nitrophenyl)-prop-2-en-1-one was synthesized and evaluated for in vitro antitubercular activity against H37R$_a$ (MTB) and *Mycobacterium bovis* BCG.[28] The active compound had a docking score of −8.267 and a Glide energy of −54.856 kcal/mol when it was docked into the active site of the

mycobacterial enoyl reductase (InhA). These outcomes piqued our interest in developing new hybrids based on the pyrazole- and pyrazoline-clubbed triazole and tetrazole pharmacophores. Herein, we reported the synthesis of a series of novel pyrazolylpyrazoline-clubbed triazole and tetrazole derivatives (9a−p) and screened them for in vitro antitubercular efficiency. The structural changes, such as replacing the oxidazole and indole moiety with a substituted pyrazoline ring, increased the pharmacological potency. Pyrazole and tetrazole were used to replace the chalcone linker between the nitrophenyl rings. The synthesized compounds showed substantial inhibition. In the active state, compound **9o** had excellent antitubercular activity against *M. tuberculosis* H$_{37}$RV, with an MIC of 12.5 μg/mL and 99% of inhibition. The docking score of the most active compound **9o** was found to be −8.884, and the Glide energy was −61.144 kcal/mol. It was found to accommodate well into the active site of InhA, engaging in a network of bonded and nonbonded interactions compared to the previously synthesized 1-(2-(1H-indol-3-yl)-5-(pyridin-4-yl)-1,3,4-oxadiazol-3(2H)-yl)-3-(2-nitrophenyl)-prop-2-en-1-one compound.

■ RESULTS AND DISCUSSION

Chemistry. The traditional synthesis pathways for novel pyrazolylpyrazoline-clubbed triazole and tetrazole derivatives (9a−p) are shown in Schemes 1 and 2.

The starting material 5-chloro-3-methyl-1-phenyl-1H-pyrazole-4-carbaldehyde (**A**) was prepared with 85% yield from the reaction of 3-methyl-1-phenyl-1H-pyrazol-5(4H)-one with DMF and POCl$_3$. 5-Chloro-4-(1,3-dioxolan-2-yl)-3-methyl-1-phenyl-1H-pyrazole (**1**) was synthesized by the reaction of derivative **A** with ethylene glycol in the presence of *p*-toluene sulfonic acid (*p*-TSA) in toluene under reflux conditions for
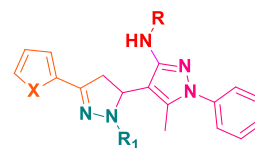
5−6 h using a Dean-Stark condenser. Compounds *N*-(4-(1,3-dioxolan-2-yl)-3-methyl-1-phenyl-1*H*-pyrazol-5-yl)-4*H*-1,2,4-triazol-4-amine (**2a**) and *N*-(4-(1,3-dioxolan-2-yl)-3-methyl-1-phenyl-1*H*-pyrazol-5-yl)-1*H*-tetrazol-5-amine (**2b**) were further synthesized from the reaction of derivative **1** with 4*H*-1,2,4-triazol-4-amine (**a**) and 1*H*-tetrazol-5-amine (**b**) in the presence of K_2CO in dry acetone at 90 °C for 2−3 h. Similarly, 5-((4*H*-1,2,4-triazol-4-yl)amino)-3-methyl-1-phenyl-1*H*-pyrazole-4-carbaldehyde (**3a**) and 5-((1*H*-tetrazol-5-yl)amino)-3-methyl-1-phenyl-1*H*-pyrazole-4-carbaldehyde (**3b**) were achieved by the deprotection of derivatives (**2a,b**) in the presence of formic acid and further reacted with 2-acetyle thiophene (**4a**) and 2-acetyle furan (**4b**) and substituted hydrazide derivatives (**5−8**) in the presence of 50% ethanolic NaOH solution at room temperature. The obtained solid precipitate was filtered, washed with ethanol, and dried in an oven at 60 °C. The products (**9a−p**) were received quantitatively in 61−91% yields with excellent purity (see Table 1).

The final structures of **9a−p** were confirmed by elemental analyses and FT-IR, ^{1}H NMR, ^{13}C NMR, and mass spectra. The purity of the compounds was checked by thin-layer chromatography (TLC). The ^{1}H NMR spectrum of derivatives **3a,b** displayed the protons of two −CH_3 groups at 2.3−2.4 ppm, and the protons of −CHO groups were exhibited near 9.9−10.2 ppm. Similarly, the ^{1}H NMR spectrum of derivatives **3a−d** showed protons of the aryl ring at 6.5−7.5 ppm. All pyrazolylpyrazoline derivatives (**9a−p**) showed characteristic absorption bands at 3341−3325 cm^{-1} due to −NH stretching. The IR spectra of derivatives **9a−p** showed expected absorption bands at 3051−3064 cm^{-1} due to aromatic C−H stretching. For the entire compound, the −C≡N stretching absorption band was observed at 1587−1620 cm^{-1}. In the ^{1}H NMR spectrum (400 MHz) of all of the synthesized compounds, the protons of the −CH_3 group were detected at 2.36−2.46 ppm. Furthermore, the CH_2 protons of the pyrazoline ring resonated as a pair of doublets of doublets near 3.21−3.29 ppm (H_a) and 3.79−3.88 ppm (H_b). The −CH (H_x) proton appeared as a doublet of doublets between 5.93 and 6.21 ppm due to vicinal coupling with the two magnetically nonequivalent protons of the methylene group at the 4th position of the pyrazoline ring. All aromatic proton (Ar−H) signals were observed between 6.96 and 7.98 ppm. In the ^{13}C NMR spectra of titled compounds (**9a−p**), one signal observed at around 55.4−56.1 ppm was attributed to the carbon of the methylene group (C_4), which confirmed the formation of the pyrazoline ring in the compounds and the molecular ion peak of the synthesized analogues with the respective molecular formulas of the compounds.

Biological Evaluation. *In Vitro Antitubercular Activity.* All prepared molecules (**9a−p**) were investigated for their in vitro antituberculosis activity as per the described process against the $H_{37}RV$ strain by the Lowenstein−Jensen slope technique with slight modification.[29] The in vitro antitubercular screening showed that the synthesized compounds exhibit good to excellent antitubercular activity in comparison to the standard drugs isoniazid and rifampicin. The results are represented in Table 2.

It was observed that compounds **9d**, **9i**, **9k**, **9l**, **9o**, and **9p** demonstrated excellent activity in terms of % inhibition, i.e., 95, 96, 98, 96, 99, and 98% at MIC (250 µg/mL), respectively. Among the series compounds, **9k** and **9o** (MIC = 12.5 µg/mL) were found to be potent compared to rifampicin (MIC =

Table 1. Synthesis of Pyrazolylpyrazoline Derivatives (9a−p)

Comp. Code	R	Hydrazine Derivatives	X	Yield (%)	Reaction Time (hr.)
9a	1,2,4-triazol-4-yl	2-aminobenzimidazole	S	79	2
9b	1,2,4-triazol-4-yl	2-aminobenzimidazole	O	82	2
9c	tetrazol-5-yl	2-aminobenzimidazole	S	77	3
9d	tetrazol-5-yl	2-aminobenzimidazole	O	72	3
9e	1,2,4-triazol-4-yl	2-aminobenzothiazole	S	89	2
9f	1,2,4-triazol-4-yl	2-aminobenzothiazole	O	91	2
9g	tetrazol-5-yl	2-aminobenzothiazole	S	83	2
9h	tetrazol-5-yl	2-aminobenzothiazole	O	81	2
9i	1,2,4-triazol-4-yl	isonicotinohydrazide	S	61	2
9j	1,2,4-triazol-4-yl	isonicotinohydrazide	O	63	2
9k	tetrazol-5-yl	isonicotinohydrazide	S	65	3
9l	tetrazol-5-yl	isonicotinohydrazide	O	72	3
9m	1,2,4-triazol-4-yl	nicotinohydrazide	S	67	2

Table 1. continued

Comp. Code	R	Hydrazine Derivatives	X	Yield (%)	Reaction Time (hr.)
9n			O	69	2
9o			S	64	3
9p			O	65	3

Table 2. In Vitro Antitubercular Activity of Compounds 9a−p against the *M. tuberculosis* H$_{37}$Rv Strain

compound no.	% inhibition, MIC (μg/mL)	compound no.	% inhibition, MIC (μg/mL)
9a	87	9j	87
9b	69	9k	98 (12.5)
9c	86	9l	96 (25)
9d	95	9m	89
9e	89	9n	86
9f	80	9o	99 (12.5)
9g	88	9p	98 (25)
9h	90	rifampicin	98 (40)
9i	96 (62.5)	isoniazid	99 (0.20)

40 μg/mL) against *M. tuberculosis* with 98 and 99% inhibition, respectively. Compounds **9l** and **9p** (MIC = 25 μg/mL) also showed good potency with 96−98% inhibition, whereas rest of the derivatives showed moderate to good antitubercular activity. It is encouraging to observe that compounds **9i**, **9l**, **9k**, **9o**, and **9p** may be optimized further to improve their potency. The remaining molecules exhibited less potency than standard drugs isoniazid and rifampicin. The graphical representation is shown in Figure 2.

Molecular Docking Study. The in silico approach of molecular docking is one of the most frequently used strategies

because of its ability to predict the conformation of small molecules within the appropriate target binding site. Therefore, to rationalize the promising level of antitubercular activity demonstrated by pyrazolylpyrazoline derivatives (**9d, 9i, 9k, 9l, 9o**, and **9p**) and gain an insight into their plausible mechanism of action, a molecular docking study was performed against mycobacterial enoyl reductase (InhA) (pdb code: 4TZK) using the GLIDE (Grid-Based Ligand Docking with Energetics) module of Schrödinger molecular modeling software (Schrödinger, LLC, New York, NY). InhA,[30] the enoyl acyl carrier protein reductase (ENR) from *M. tuberculosis*, is one of the key enzymes contributing to mycolic acid biosynthesis, which is a major component of the bacterial cell wall. Inhibition of InhA disrupts the integrity of the mycobacterial cell wall and thus qualifies it as the promising target of novel antimycobacterial drugs.[31] All of the six compounds (**9d, 9i, 9k, 9l, 9o**, and **9p**) were docked in the binding site of InhA and displayed a good binding affinity with docking scores in the range from −8.884 to −7.113 (Table 3).

Table 3. Molecular Docking of Novel Compounds in the Active Site of MTB Enoyl Reductase (InhA)

comp. code	glide score	glide energy (kcal/mol)	H-bonding (Å)	Pi−Pi stacking (Å)
9d	−7.113	−50.544	Tyr158(2.501)	
9i	−7.599	−52.058	Lys165(1.996)	Tyr158(2.221)
9k	−8.514	−60.464	Lys165(2.275)	Tyr158(1.900)
9l	−7.892	−54.284	Lys165(2.090)	Tyr158(1.885)
9o	−8.884	−61.144	Lys165(2.220)	Tyr158(1.912)
9p	−7.982	−55.463	Lys165(2.072)	Tyr158(1.913)

A detailed analysis of the per-residue interactions for one of the most active analogues (**9o**) could help to identify the most significantly interacting residues and the type of thermodynamic interactions that govern its binding to the target, which is elaborated in the next section. The lowest energy docked conformation of **9o** (Glide score: −8.884 and Glide binding energy: −61.144 kcal/mol) was found to be snugly bound to the active site of InhA through significant bonded and nonbonded interactions (Figure 3). The predicted binding mode of **9o** suggested that the observed potency may be due to the extensive van der Waals interactions with Leu218
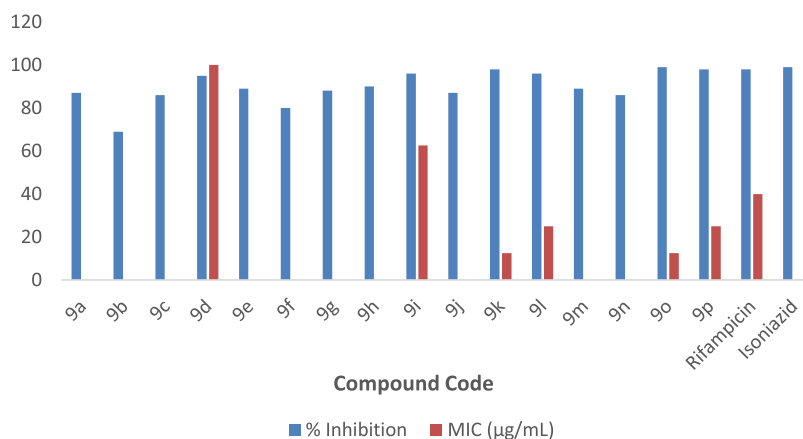
In vitro antitubercular activity of (9a-p)

Figure 2. Graphical representation of antibacterial activity.

Figure 3. Binding mode and interactions of **9o** into the active site of mycobacterial InhA (on the right side: the green line represents the pi–pi stacking interactions).

Figure 4. Binding mode and interactions of **9k** into the active site of mycobacterial InhA (on the right side: the green line represents the pi–pi stacking interactions).

(−1.46 kcal/mol), Ile215 (−2.247 kcal/mol), Met199 (−4.375 kcal/mol), Pro193 (−1.843 kcal/mol), Gly192 (−1.714 kcal/mol), Ala191 (−1.64 kcal/mol), Tyr158 (−2.674 kcal/mol), Ala157 (−1.303 kcal/mol), Met155 (−1.375 kcal/mol), Phe149 (−6.041 kcal/mol), Asp148 (−1.597 kcal/mol), and Met147 (−3.952 kcal/mol) through the 5-(thiophen-2-yl)−3,4-dihydro-1-(pyridin-3-yl) pyrazole section, while the 3′-((1*H*-tetrazol-5-yl)amino)−5′-methyl-1′-phenyl-substituted pyrazole section was engaged in similar type of interactions with Ile202 (−1.224 kcal/mol), Ala198 (−1.248 kcal/mol), Thr196 (−2.63 kcal/mol), Ile194 (−2.084 kcal/mol), Lys165 (−1.847 kcal/mol), Met161 (−3.041 kcal/mol), Met103 (−2.241 kcal/mol), Met98 (−1.865 kcal/mol), Phe97 (−3.378 kcal/mol), Gly96 (−3.967 kcal/mol), Ser94 (−1.785 kcal/mol), and Ile21 (−1.932 kcal/mol) residues of active sites. The enhanced binding affinity is also attributed to favorable electrostatic interactions with Glu219 (−1.458 kcal/mol), Glu210 (−1.324 kcal/mol), Met199 (−1.285 kcal/mol), Ala191 (−1.233 kcal/mol), Lys165 (−5.043 kcal/mol), Met161 (−1.062 kcal/mol), Tyr158 (−1.342 kcal/mol), Asp150 (−1.169 kcal/mol), and Ile95 (−2.457 kcal/mol). Further, it was observed to interact with the side chain of Lys165 via hydrogen bonding between nitrogen atoms of the tetrazole group. Apart from these interactions, it was further stabilized by pi–pi interactions with Tyr158. Such hydrogen

bonding and pi–pi stacking interactions "anchor" the ligand into the 3D space of the active site and further facilitate the steric and electrostatic interactions. Even the other active compound **9k** also exhibited such bonded and nonbonded interactions, which could stabilize the molecules into the active site of InhA (Figure 4).

■ CONCLUSIONS

Optimization of the titled compounds will be important in the development of new antitubercular drugs in the upcoming years. Conventional synthesis and the hybrid molecule idea were used to develop the active analogues. The salient features of this green protocol are the one-pot reaction, short reaction time, and straightforward workup procedure. The majority of the derivatives were produced in good yields with high purity. The inclusion of electron-withdrawing and -donating groups in compounds **9l**, **9k**, **9o**, and **9p** resulted in excellent antitubercular activity. The pyrazolylpyrazoline derivatives may fit well into the active site of InhA, forming significant bonded and nonbonded interactions, according to molecular docking studies. These in silico findings, which are validated by in vitro antitubercular outcomes, provide a foundation for continuing the structure-based drug design approach to uncover potent leads with better selectivity. The fact that compound **9o** with isoniazid, thiol link, and 2-acetylfuran

compound fused with the pyrazole and pyrazoline ring has outstanding antitubercular activity and a high docking score motivated us to develop new hybrids based on the core structure and explore their antitubercular activity.

■ EXPERIMENTAL SECTION

Materials and Methods. All reactions were performed with analytical grade reagents (Sigma-Aldrich), which were used without further purification. The progress of reactions was monitored by thin-layer chromatography (TLC) on aluminum plates coated with silica gel 60 F254 (layer thickness 0.25 mm; Merck); components were detected by exposure to UV light or iodine vapor. The melting points were determined in open capillary tubes on an electrothermal melting point apparatus. The IR spectra were recorded in KBr on a Perkin Elmer FT-IR spectrophotometer ($490-8500$ cm^{-1}). The ^{1}H NMR and ^{13}C NMR spectra were recorded in DMSO-d_6 on a Bruker Advance 400 spectrometer at 400 and 100 MHz, respectively, using DMSO-d_6 as a solvent and TMS as an internal standard. Chemical shifts are reported in parts per million (ppm). Elemental analysis (% C, H, N) was performed using a Perkin Elmer 2400 Series II elemental analyzer. A mass spectrum was scanned on a Shimadzu LC−MS 2010 spectrophotometer.

Preparation of 5-Chloro-4-(1,3-dioxolan-2-yl)-3-methyl-1-phenyl-1H-pyrazole (1). A mixture of the starting material 5-chloro-3-methyl-1-phenyl-1*H*-pyrazole-4-carbaldehyde (**A**, 30 mmol), toluene (25 mL), and ethylene glycol (45 mmol) was put into a 100 mL RBF. To this solution, a catalytic amount of *p*-toluene sulfonic acid (*p*-TSA, 1.5 mmol) was added, and the reaction mixture was heated under reflux for 5−6 h by a Dean-Stark condenser. Completion of the reactions was monitored by TLC (ethyl acetate/petroleum ether 1:9). After removal of the solvent under reduced pressure, water was added to the reaction mixture, and then the aqueous layer was extracted twice with ethyl acetate. The combined organic layer was dried over sodium sulfate, and ethyl acetate was evaporated under vacuum to obtain 5-chloro-4-(1,3-dioxolan-2-yl)-3-methyl-1-phenyl-1*H*-pyrazole (**1**) with 90% yield. The obtained crude material was directly used for the next step without further purification.

Preparation of N-(4-(1,3-Dioxolan-2-yl)-3-methyl-1-phenyl-1H-pyrazol-5-yl)-4H-1,2,4-triazol-4-amine (2a) and N-(4-(1,3-Dioxolan-2-yl)-3-methyl-1-phenyl-1H-pyrazol-5-yl)-1H-tetrazol-5-amine (2b). In a three-neck RBF, 0.1 mol of compound **1** was added to dry acetone (60 mL), followed by addition of 0.15 mol of anhydrous K$_2$CO$_3$. After that, 0.11 mol of 4*H*-1,2,4-triazol-4-amine (**a**) or 1*H*-tetrazol-5-amine (**b**) was added to the above reaction mass. The mixture was stirred at 90 °C for 2−3 h. The progress of the reaction was monitored by TLC. The product mass was added to cold water, followed by extraction with ethyl acetate. The organic layer was dried over sodium sulfate and evaporated under reduced pressure to achieve compounds **2a,b** in good yields (84−87%).

Preparation of 5-((4H-1,2,4-Triazol-4-yl)amino)-3-methyl-1-phenyl-1H-pyrazole-4-carbaldehyde (3a) and 5-((1H-Tetrazol-5-yl)amino)-3-methyl-1-phenyl-1H-pyrazole-4-carbaldehyde (3b). In a 50 mL three-neck RBF, compounds **2a,b** (2.0 g) were added, followed by formic acid (10 mL), and refluxed for 30 min. Excess of formic acid was removed by evaporation under reduced pressure, and the residue was portioned between saturated, aqueous sodium carbonate and ethyl acetate. The organic phase was dried over sodium sulfate

and evaporated to dryness to leave the crude product. The crude product was purified by silica gel column chromatography (mobile phase 1−3% ethyl acetate in petroleum ether). The pure product was obtained in 78−83% yield.

General Procedure for the Synthesis of Pyrazolylpyrazoline-Clubbed Triazole and Tetrazole Derivatives (9a−p). In a 250 mL RBF, derivatives **3a,b** (5 mmol) and derivatives **4a,b** were added to a solution of substituted hydrazide derivatives (**5−8**, 5.5 mmol) in a 50% ethanolic NaOH solution (50 mL) and the reaction mass was stirred for 2−3 h at RT. Obtained solid precipitates were filtered, washed with ethanol, and dried in an oven at 60 °C. The final products (**9a−p**) were received quantitatively in 61−91% yields with excellent purity. All synthesized compounds were well characterized through different spectroscopic techniques, and characterization data for all synthesized compounds (**9a−p**) are given below.

Characterization of 2-(1H-Benzo[d]imidazol-2-yl)-5′-methyl-1′-phenyl-5-(thiophen-2-yl)-N-(4H-1,2,4-triazol-4-yl)-3,4-dihydro-1′H,2H-[3,4′-bipyrazol]-3′-amine (9a). Yield 79%, mp 225−226 °C; IR (KBr) λ_{max}: 3350 (N−H stretching), 3320 (N−H stretching), 3062 (Ar−CH stretching), 2925 (C−H aliphatic stretching), 1610 (C═C stretching), 1599 (C═N), 760 (−S-linkage); ^{1}H NMR (DMSO-d_6, 400 MHz): 1.81 (dd, 1H, CH$_2$ group), 1.86 (dd, 1H, CH$_2$ group), 1.89 (dd, 1H, CH group), 2.30 (s, 3H, −CH$_3$), 5.16 (s, 1H, −NH), 6.04 (s, 1H, NH), 7.07−7.96 (m, 14H, Ar−H); ^{13}C NMR (DMSO-d_6, 100 MHz): 21.3, 43.4, 56.0, 115.2, 115.4, 115.8, 120.2, 120.8, 121.6, 121.7, 122.2, 124.2, 125.9, 127.0, 127.2, 128.2, 128.3, 128.5, 130.4, 130.8, 131.9, 133.3, 135.0, 148.8, 150.0, 152.2; LCMS: m/z = 507.10 (M$^+$); anal. calcd for C$_{26}$H$_{22}$N$_{10}$S: C, 61.64; H, 4.38; N, 27.65%; found: C, 61.96; H, 4.52; N, 27.68%.

Characterization of 2-(1H-Benzo[d]imidazol-2-yl)-5-(furan-2-yl)-5′-methyl-1′-phenyl-N-(4H-1,2,4-triazol-4-yl)-3,4-dihydro-1′H,2H-[3,4′-bipyrazol]-3′-amine (9b). Yield 82%, mp 227−228 °C; IR (KBr) λ_{max}: 3350 (N−H stretching), 3321 (N−H stretching), 3058 (Ar−CH stretching), 2950 (C−H aliphatic stretching), 1605 (C═C stretching), 1599 (C═N), 759 (−S-linkage); ^{1}H NMR (DMSO-d_6, 400 MHz): 1.81 (dd, 1H, CH$_2$ group), 1.86 (dd, 1H, CH$_2$ group), 1.88 (dd, 1H, CH group), 2.30 (s, 3H, −CH$_3$), 5.14 (s, 1H, −NH), 6.05 (s, 1H, NH), 7.07−8.10 (m, 14H, Ar−H); ^{13}C NMR (DMSO-d_6, 100 MHz): 21.4, 43.4, 56.0, 115.4, 115.6, 115.9, 120.2, 120.8, 121.6, 121.7, 122.2, 124.2, 125.9, 127.0, 128.0, 128.2, 128.3, 128.5, 130.4, 130.9, 131.9, 133.3, 135.0, 148.8, 150.0, 152.4; LCMS: m/z = 491.2 (M$^+$); anal. calcd for C$_{26}$H$_{22}$N$_{10}$O: C, 63.66; H, 4.52; N, 28.55%; found: C, 63.26; H, 4.60; N, 28.52%.

Characterization of 2-(1H-Benzo[d]imidazol-2-yl)-5′-methyl-1′-phenyl-N-(1H-tetrazol-5-yl)-5-(thiophen-2-yl)-3,4-dihydro-1′H,2H-[3,4′-bipyrazol]-3′-amine (9c). Yield 77%, mp 228−230 °C; IR (KBr) λ_{max}: 3345 (N−H stretching), 3340 (N−H stretching), 3321 (N−H stretching), 3058 (Ar−CH stretching), 2950 (C−H aliphatic stretching), 1605 (C═C stretching), 1599 (C═N), 759 (−S-linkage); ^{1}H NMR (DMSO-d_6, 400 MHz): 1.83 (dd, 1H, CH$_2$ group), 1.84 (dd, 1H, CH$_2$ group), 1.85 (dd, 1H, CH group), 2.30 (s, 3H, −CH$_3$), 5.16 (s, 1H, −NH), 5.18 (s, 1H, −NH), 6.06 (s, 1H, NH), 7.10−8.10 (m, 12H, Ar−H); ^{13}C NMR (DMSO-d^6, 100 MHz): 20.3, 44.4, 56.0, 113.2, 115.4, 115.8, 120.2, 120.8, 121.6, 121.7, 122.2, 124.2, 125.9, 127.0, 127.2, 128.2, 128.3, 128.5, 130.4, 131.8, 131.9, 133.3, 135.2, 148.8, 163.4; LCMS:

m/z = 507.10 (M$^+$); anal. calcd for C$_{25}$H$_{21}$N$_{11}$S: C, 59.16; H, 4.17; N, 30.36%; found: C, 59.20; H, 4.20; N, 30.34%.

Characterization of 2-(1H-Benzo[d]imidazol-2-yl)-5-(furan-2-yl)-5′-methyl-1′-phenyl-N-(1H-tetrazol-5-yl)-3,4-dihydro-1′H,2H-[3,4′-bipyrazol]-3′-amine (9d). Yield 72%, mp 225−226 °C; IR (KBr) λ_{max}: 3345 (N−H stretching), 3340 (N−H stretching), 3321 (N−H stretching), 3058 (Ar−CH stretching), 3058 (Ar−CH), 1605 (C=C stretching), 1599 (C=N), 759 (−S-linkage); ^{1}H NMR (DMSO-d_6, 400 MHz): 1.82 (dd, 1H, CH$_2$ group), 1.86 (dd, 1H, CH$_2$ group), 1.87 (dd, 1H, CH group), 2.30 (s, 3H, −CH$_3$), 5.16 (s, 1H, −NH), 5.18 (s, 1H, −NH), 6.05 (s, 1H, NH), 7.07−8.10 (m, 12H, Ar−H); ^{13}C NMR (DMSO-d_6, 100 MHz): 22.3, 44.4, 56.0, 113.2, 115.4, 116.8, 120.2, 120.8, 121.6, 121.7, 122.2, 124.2, 125.9, 127.0, 127.4, 128.2, 128.3, 128.5, 130.4, 131.4, 131.9, 133.3, 135.2, 146.8, 162.4; LCMS: m/z = 491.20 (M$^+$); anal. calcd for C$_{25}$H$_{21}$N$_{11}$O: C, 61.09; H, 4.31; N, 31.35%; found: C, 61.20; H, 4.20; N, 31.34%.

Characterization of 2-(Benzo[d]thiazol-2-yl)-5′-methyl-1′-phenyl-5-(thiophen-2-yl)-N-(4H-1,2,4-triazol-4-yl)-3,4-dihydro-1′H,2H-[3,4′-bipyrazol]-3′-amine (9e). Yield 89%, mp 235−236 °C; IR (KBr) λ_{max}: 3321 (N−H stretching), 3058 (Ar−CH stretching), 2950 (C−H aliphatic stretching), 1605 (C=C stretching), 1599 (C=N), 759 (−S-linkage); ^{1}H NMR (DMSO-d_6, 400 MHz): 1.82 (dd, 1H, CH$_2$ group), 1.82 (dd, 1H, CH$_2$ group), 1.89 (dd, 1H, CH group), 2.31 (s, 3H, −CH$_3$), 5.16 (s, 1H, −NH), 7.07−7.96 (m, 14H, Ar−H); ^{13}C NMR (DMSO-d_6, 100 MHz): 22.3, 42.4, 56.0, 115.2, 115.4, 116.8, 120.2, 120.8, 121.6, 121.7, 122.2, 124.2, 125.9, 127.0, 127.3, 128.2, 128.3, 128.5, 130.4, 130.8, 131.9, 133.3, 135.0, 148.8, 150.0, 152.4; LCMS: m/z = 523.10 (M$^+$); anal. calcd for C$_{26}$H$_{21}$N$_9$S$_2$: C, 59.64, H, 4.04; N, 24.07%; found: C, 59.66; H, 4.10; N, 24.48%.

Characterization of 2-(Benzo[d]thiazol-2-yl)-5-(furan-2-yl)-5′-methyl-1′-phenyl-N-(4H-1,2,4-triazol-4-yl)-3,4-dihydro-1′H,2H-[3,4′-bipyrazol]-3′-amine (9f). Yield 91%, mp 229−230 °C; IR (KBr) λ_{max}: 3322 (N−H stretching), 3060 (Ar−CH stretching), 2940 (C−H aliphatic stretching), 1610 (C=C stretching), 1599 (C=N), 760 (−S-linkage); ^{1}H NMR (DMSO-d_6, 400 MHz): 1.81 (dd, 1H, CH$_2$ group), 1.83 (dd, 1H, CH$_2$ group), 1.88 (dd, 1H, CH group), 2.30 (s, 3H, −CH$_3$), 5.16 (s, 1H, −NH), 7.06−7.92 (m, 14H, Ar−H); ^{13}C NMR (DMSO-d_6, 100 MHz): 23.4, 42.4, 56.0, 115.4, 115.4, 115.9, 121.2, 120.8, 121.6, 121.7, 122.2, 124.2, 125.9, 127.0, 127.4, 128.2, 128.3, 128.5, 130.4, 130.9, 131.9, 134.3, 135.0, 148.8, 150.0, 152.4; LCMS: m/z = 507.10 (M$^+$); anal. calcd for C$_{26}$H$_{21}$N$_9$OS: C, 61.52; H, 4.17; N, 24.84%; found: C, 61.26; H, 4.52; N, 24.52%

Characterization of 2-(Benzo[d]thiazol-2-yl)-5′-methyl-1′-phenyl-N-(1H-tetrazol-5-yl)-5-(thiophen-2-yl)-3,4-dihydro-1′H,2H-[3,4′-bipyrazol]-3′-amine (9g). Yield 83%, mp 220−221 °C; IR (KBr) λ_{max}: 3340 (N−H stretching), 3321 (N−H stretching), 3058 (Ar−CH stretching), 2950 (C−H aliphatic stretching), 1605 (C=C stretching), 1599 (C=N), 759 (−S-linkage); ^{1}H NMR (DMSO-d_6, 400 MHz): 1.81 (dd, 1H, CH$_2$ group), 1.82 (dd, 1H, CH$_2$ group), 1.85 (dd, 1H, CH group), 2.30 (s, 3H, −CH$_3$), 5.16 (s, 1H, −NH), 5.18 (s, 1H, −NH), 7.10−8.10 (m, 12H, Ar−H); ^{13}C NMR (DMSO-d_6, 100 MHz): 21.3, 44.4, 54.0, 112.2, 115.4, 115.8, 120.2, 120.8, 121.6, 121.7, 122.2, 124.2, 125.9, 127.0, 127.4, 128.2, 128.3, 128.5, 130.4, 131.8, 131.9, 133.3, 135.2, 148.8, 160.4; LCMS: m/z = 524.2 (M$^+$); anal. calcd for C$_{25}$H$_{20}$N$_{10}$S$_2$: C, 57.24; H, 3.84; N, 26.70%; found: C, 57.20; H, 3.85; N, 26.75%.

Characterization of 2-(Benzo[d]thiazol-2-yl)-5-(furan-2-yl)-5′-methyl-1′-phenyl-N-(1H-tetrazol-5-yl)-3,4-dihydro-1′H,2H-[3,4′-bipyrazol]-3′-amine (9h). Yield 81%, mp 221−223 °C; IR (KBr) λ_{max}: 3340 (N−H stretching), 3322 (N−H stretching), 3057 (Ar−CH stretching), 2950 (C−H aliphatic stretching), 1604 (C=C stretching), 1597 (C=N), 759 (−S-linkage); ^{1}H NMR (DMSO-d_6, 400 MHz): 1.82 (dd, 1H, CH$_2$ group), 1.86 (dd, 1H, CH$_2$ group), 1.87 (dd, 1H, CH group), 2.30 (s, 3H, −CH$_3$), 5.16 (s, 1H, −NH), 5.18 (s, 1H, −NH), 6.05 (s, 1H, NH), 7.07−8.10 (m, 12H, Ar−H); ^{13}C NMR (DMSO-d_6, 100 MHz): 21.3, 44.4, 55.0, 113.2, 115.4, 116.8, 120.2, 120.8, 121.6, 121.7, 122.2, 124.2, 125.9, 127.0, 127.2, 128.2, 128.3, 128.5, 130.4, 131.4, 131.9, 133.3, 135.2, 147.8, 160.3; LCMS: m/z = 509.1 (M$^+$); anal. calcd for C$_{25}$H$_{20}$N$_{10}$SO: C, 59.04; H, 3.96; N, 27.54%; found: C, 59.20; H, 3.90; N, 27.75%.

Characterization of 3′-((4H-1,2,4-Triazol-4-yl)amino)-5′-methyl-1′-phenyl-5-(thiophen-2-yl)-3,4-dihydro-1′H,2H-[3,4′-bipyrazol]-2-yl)(pyridin-4-yl)methanone (9i). Yield 61%, mp 234−235 °C; IR (KBr) λ_{max}: 3321 (N−H stretching), 3058 (Ar−CH stretching), 2952 (C−H aliphatic stretching), 1680 (CONH stretching), 1605 (C=C stretching), 1599 (C=N), 759 (−S-linkage); ^{1}H NMR (DMSO-d_6, 400 MHz): 1.82 (dd, 1H, CH$_2$ group), 1.82 (dd, 1H, CH$_2$ group), 1.89 (dd, 1H, CH group), 2.32 (s, 3H, −CH$_3$), 5.16 (s, 1H, −NH), 7.07−7.96 (m, 14H, Ar−H); ^{13}C NMR (DMSO-d_6, 100 MHz): 20.3, 42.4, 57.0, 113.2, 115.4, 116.8, 120.2, 120.8, 121.6, 121.7, 122.2, 124.2, 125.9, 127.0, 127.4, 128.2, 128.3, 128.5, 130.4, 131.4, 131.9, 133.3, 135.2, 146.8, 162.4; LCMS: m/z = 495.20 (M$^+$); anal. calcd for C$_{25}$H$_{21}$N$_9$SO: C, 60.59, H, 4.27; N, 25.44%; found: C, 60.66; H, 4.30; N, 25.48%.

Characterization of (3′-((4H-1,2,4-Triazol-4-yl)amino)-5-(furan-2-yl)-5′-methyl-1′-phenyl-3,4-dihydro-1′H,2H-[3,4′-bipyrazol]-2-yl)(pyridin-4-yl)methanone (9j). Yield 63%, mp 233−234 °C; IR (KBr) λ_{max}: 3320 (N−H stretching), 3057 (Ar−CH stretching), 2950 (C−H aliphatic stretching), 1670 (CONH stretching), 1605 (C=C stretching), 1599 (C=N), 759 (−S-linkage); ^{1}H NMR (DMSO-d_6, 400 MHz): 1.81 (dd, 1H, CH$_2$ group), 1.82 (dd, 1H, CH$_2$ group), 1.89 (dd, 1H, CH group), 2.30 (s, 3H, −CH$_3$), 5.16 (s, 1H, −NH), 7.07−7.97 (m, 14H, Ar−H); ^{13}C NMR (DMSO-d_6, 100 MHz): 22.3, 43.4, 57.0, 113.2, 116.4, 116.8, 121.2, 121.8, 122.6, 123.7, 124.0, 124.2, 125.9, 127.0, 127.4, 128.2, 128.3, 128.5, 130.4, 131.4, 131.9, 133.3, 135.2, 146.8, 161.3; LCMS: m/z = 480.2 (M$^+$); anal. calcd for C$_{25}$H$_{21}$N$_9$O$_2$: C, 62.62, H, 4.41; N, 26.29%; found: C, 62.66; H, 4.42; N, 26.48%.

Characterization of (3′-((1H-Tetrazol-5-yl)amino)-5′-methyl-1′-phenyl-5-(thiophen-2-yl)-3,4-dihydro-1′H,2H-[3,4′-bipyrazol]-2-yl)(pyridin-4-yl)methanone (9k). Yield 65%, mp 238−240 °C; IR (KBr) λ_{max}: 3340 (N−H stretching), 3321 (N−H stretching), 3058 (Ar−CH stretching), 2950 (C−H aliphatic stretching), 1675 (CONH stretching), 1605 (C=C stretching), 1599 (C=N), 759 (−S-linkage); ^{1}H NMR (DMSO-d_6, 400 MHz): 1.82 (dd, 1H, CH$_2$ group), 1.83 (dd, 1H, CH$_2$ group), 1.85 (dd, 1H, CH group), 2.31 (s, 3H, −CH$_3$), 5.16 (s, 1H, −NH), 5.18 (s, 1H, −NH), 7.10−8.10 (m, 12H, Ar−H); ^{13}C NMR (DMSO-d_6, 100 MHz): 20.3, 42.4, 57.0, 113.2, 115.4, 117.8, 120.2, 120.8, 121.6, 121.7, 123.2, 124.2, 125.9, 127.0, 127.4, 129.2, 129.3, 129.5, 130.4, 131.4, 132.9, 134.3, 135.2, 160.8; LCMS: m/z = 497.2 (M$^+$); anal. calcd for C$_{24}$H$_{20}$N$_{10}$SO: C, 58.05; H, 4.06; N, 28.21%; found: C, 58.20; H, 4.10; N, 28.25%.

Characterization of (3′-((1H-Tetrazol-5-yl)amino)-5-(furan-2-yl)-5′-methyl-1′-phenyl-3,4-dihydro-1′H,2H-[3,4′-bipyrazol]-2-yl)(pyridin-4-yl)methanone (9l). Yield 72%, mp 236−237 °C; IR (KBr) λ_{max}: 3341 (N−H stretching), 3331 (N−H stretching), 3048 (Ar−CH stretching), 2950 (C−H aliphatic stretching), 1670 (CONH stretching), 1605 (C=C stretching), 1599 (C=N), 759 (−S-linkage); ^{1}H NMR (DMSO-d^6, 400 MHz): 1.81 (dd, 1H, CH$_2$ group), 1.83 (dd, 1H, CH$_2$ group), 1.85 (dd, 1H, CH group), 2.30 (s, 3H, −CH$_3$), 5.16 (s, 1H, −NH), 5.18 (s, 1H, −NH), 7.10−8.10 (m, 12H, Ar−H); ^{13}C NMR (DMSO-d^6, 100 MHz): 20.4, 42.4, 57.0, 113.2, 115.4, 117.8, 120.2, 120.8, 121.6, 121.7, 122.2, 124.2, 125.9, 127.0, 127.4, 129.2, 129.3, 129.5, 130.4, 131.4, 132.9, 133.3, 134.2, 158.8; LCMS: m/z = 481.2 (M$^+$); anal. calcd for C$_{24}$H$_{20}$N$_{10}$O$_2$: C, 59.99; H, 4.20; N, 29.15%; found: C, 59.90; H, 4.15; N, 29.25%.

Characterization of (3′-((4H-1,2,4-Triazol-4-yl)amino)-5′-methyl-1′-phenyl-5-(thiophen-2-yl)-3,4-dihydro-1′H,2H-[3,4′-bipyrazol]-2-yl)(pyridin-3-yl)methanone (9m). Yield 67%, mp 234−235 °C; IR (KBr) λ_{max}: 3321 (N−H stretching), 3058 (Ar−CH stretching), 2952 (C−H aliphatic stretching), 1680 (CONH stretching), 1605 (C=C stretching), 1599 (C=N), 759 (−S-linkage); ^{1}H NMR (DMSO-d^6, 400 MHz): 1.82 (dd, 1H, CH$_2$ group), 1.82 (dd, 1H, CH$_2$ group), 1.89 (dd, 1H, CH group), 2.32 (s, 3H, −CH$_3$), 5.16 (s, 1H, −NH), 7.07−7.96 (m, 14H, Ar−H); ^{13}C NMR (DMSO-d^6, 100 MHz): 22.3, 44.4, 57.0, 114.2, 115.4, 116.8, 120.2, 120.8, 121.6, 121.7, 123.2, 124.2, 125.9, 127.0, 127.4, 128.2, 128.3, 128.5, 130.4, 131.4, 131.9, 133.3, 135.2, 146.8, 162.4; LCMS: m/z = 495.20 (M$^+$); anal. calcd for C$_{25}$H$_{21}$N$_9$SO: C, 60.59, H, 4.27; N, 25.44%; found: C, 60.64; H, 4.31; N, 25.46%.

Characterization of (3′-((4H-1,2,4-Triazol-4-yl)amino)-5-(furan-2-yl)-5′-methyl-1′-phenyl-3,4-dihydro-1′H,2H-[3,4′-bipyrazol]-2-yl)(pyridin-3-yl)methanone (9n). Yield 69%, mp 233−234 °C; IR (KBr) λ_{max}: 3320 (N−H stretching), 3057 (Ar−CH stretching), 2950 (C−H aliphatic stretching), 1670 (CONH stretching), 1605 (C=C stretching), 1599 (C=N), 759 (−S-linkage); ^{1}H NMR (DMSO-d^6, 400 MHz): 1.81 (dd, 1H, CH$_2$ group), 1.82 (dd, 1H, CH$_2$ group), 1.89 (dd, 1H, CH group), 2.30 (s, 3H, −CH$_3$), 5.16 (s, 1H, −NH), 7.07−7.97 (m, 14H, Ar−H); ^{13}C NMR (DMSO-d^6, 100 MHz): 22.4, 43.4, 57.0, 113.2, 116.4, 117.8, 120.2, 120.8, 122.6, 123.7, 123.9, 124.2, 125.9, 127.0, 127.4, 128.2, 128.3, 128.5, 130.4, 131.4, 131.9, 133.3, 135.2, 146.8, 161.3; LCMS: m/z = 480.2 (M$^+$); anal. calcd for C$_{25}$H$_{21}$N$_9$O$_2$: C, 62.62, H, 4.41; N, 26.29%; found: C, 62.66; H, 4.42; N, 26.48%.

Characterization of (3′-((1H-Tetrazol-5-yl)amino)-5′-methyl-1′-phenyl-5-(thiophen-2-yl)-3,4-dihydro-1′H,2H-[3,4′-bipyrazol]-2-yl)(pyridin-3-yl)methanone (9o). Yield 64%, mp 238−239 °C; IR (KBr) λ_{max}: 3340 (N−H stretching), 3321 (N−H stretching), 3058 (Ar−CH stretching), 2950 (C−H aliphatic stretching), 1675 (CONH stretching), 1605 (C=C stretching), 1599 (C=N), 759 (−S-linkage); ^{1}H NMR (DMSO-d^6, 400 MHz): 1.82 (dd, 1H, CH$_2$ group), 1.83 (dd, 1H, CH$_2$ group), 1.85 (dd, 1H, CH group), 2.31 (s, 3H, −CH$_3$), 5.16 (s, 1H, −NH), 5.18 (s, 1H, −NH), 7.10−8.10 (m, 12H, Ar−H); ^{13}C NMR (DMSO-d^6, 100 MHz): 21.3, 44.4, 57.0, 113.2, 115.4, 117.8, 121.4, 121.6, 121.7, 122.2, 123.2, 124.2, 125.9, 127.0, 127.4, 129.2, 129.3, 129.5, 130.4, 131.4, 132.9, 134.3, 135.2, 161.8; LCMS: m/z = 497.2 (M$^+$); anal. calcd for C$_{24}$H$_{20}$N$_{10}$SO: C, 58.05; H, 4.06; N, 28.21%; found: C, 58.20; H, 4.10; N, 28.25%.

Characterization of (3′-((1H-Tetrazol-5-yl)amino)-5-(furan-2-yl)-5′-methyl-1′-phenyl-3,4-dihydro-1′H,2H-[3,4′-bipyrazol]-2-yl)(pyridin-3-yl)methanone (9p). Yield 65%, mp 236−238 °C; IR (KBr) λ_{max}: 3341 (N−H stretching), 3331 (N−H stretching), 3048 (Ar−CH stretching), 2950 (C−H aliphatic stretching), 1670 (CONH stretching), 1605 (C=C stretching), 1599 (C=N), 759 (−S-linkage); ^{1}H NMR (DMSO-d^6, 400 MHz): 1.81 (dd, 1H, CH$_2$ group), 1.83 (dd, 1H, CH$_2$ group), 1.85 (dd, 1H, CH group), 2.30 (s, 3H, −CH$_3$), 5.16 (s, 1H, −NH), 5.18 (s, 1H, −NH), 7.10−8.10 (m, 12H, Ar−H); ^{13}C NMR (DMSO-d^6, 100 MHz): 21.4, 43.4, 57.0, 113.2, 115.4, 117.8, 120.2, 120.8, 121.6, 121.9, 122.2, 124.2, 125.9, 127.0, 127.4, 129.2, 129.3, 129.5, 130.4, 131.4, 132.9, 133.3, 134.2, 159.8; LCMS: m/z = 481.1 (M$^+$); anal. calcd for C$_{24}$H$_{20}$N$_{10}$O$_2$: C, 59.99; H, 4.20; N, 29.15%; found: C, 59.90; H, 4.15; N, 29.25%.

■ ASSOCIATED CONTENT

Ⓢ Supporting Information

The Supporting Information is available free of charge at https://pubs.acs.org/doi/10.1021/acsomega.2c07267.

Additional figures illustrating the characterization of synthesized compounds by ^{1}H NMR, ^{13}C NMR, mass, and IR spectra; methodology for the biological assay; and molecular docking study (PDF)

■ AUTHOR INFORMATION

Corresponding Author

Mayursinh Zala − *Department of Chemistry, Faculty of Science, M.G. Science Institute, Affiliated with Gujarat University, Ahmedabad 380009, India;* ⓞ orcid.org/0000-0003-3873-7756; Email: zalamayursinh2794@gamil.com

Authors

Jwalant J. Vora − *Department of Chemistry, Faculty of Science, M.G. Science Institute, Affiliated with Gujarat University, Ahmedabad 380009, India*

Vijay M. Khedkar − *Department of Pharmaceutical Chemistry, School of Pharmacy, Vishwakarma University, Pune 424001 Maharashtra, India*

Complete contact information is available at:
https://pubs.acs.org/10.1021/acsomega.2c07267

Notes

The authors declare no competing financial interest.

■ REFERENCES

(1) TB Reports. https://www.who.int/teams/global-tuberculosis-programme/tb-reports (accessed Sept 5, 2021).

(2) Lange, C.; Dheda, K.; Chesov, D.; Mandalakas, A. M.; Udwadia, Z.; Horsburgh, C. R. Management of Drug-Resistant Tuberculosis. *Lancet* **2019**, *394*, 953−966.

(3) Desai, N. C.; Bhatt, K.; Monapara, J.; Pandit, U.; Khedkar, V. M. Conventional and Microwave-Assisted Synthesis, Antitubercular Activity, and Molecular Docking Studies of Pyrazole and Oxadiazole Hybrids. *ACS Omega* **2021**, *6*, 28270−28284.

(4) Dai, H.; Huang, M.; Qian, J.; Liu, J.; Meng, C.; Li, Y.; Ming, G.; Zhang, T.; Wang, S.; Shi, Y.; Yao, Y.; Ge, S.; Zhang, Y.; Ling, Y. Excellent Antitumor and Antimetastatic Activities Based on Novel Coumarin/Pyrazole Oxime Hybrids. *Eur. J. Med. Chem.* **2019**, *166*, 470−479.

(5) Ghasempour, L.; Asghari, S.; Tajbakhsh, M.; Mohseni, M. Preparation of New Spiropyrazole, Pyrazole and Hydantoin Derivatives and Investigation of Their Antioxidant and Antibacterial Activities. *Chem. Biodiversity* **2021**, *18*, No. e2100197.

(6) Negri, A.; Javidnia, P.; Mu, R.; Zhang, X.; Vendome, J.; Gold, B.; Roberts, J.; Barman, D.; Ioerger, T.; Sacchettini, J. C.; Jiang, X.; Burns-Huang, K.; Warrier, T.; Ling, Y.; Warren, J. D.; Oren, D. A.; Beuming, T.; Wang, H.; Wu, J.; Li, H.; Rhee, K. Y.; Nathan, C. F.; Liu, G.; Somersan-Karakaya, S. Identification of a Mycothiol-Dependent Nitroreductase from *Mycobacterium Tuberculosis*. *ACS Infect. Dis.* **2018**, *4*, 771−787.

(7) Liu, J.-J.; Zhao, M.; Zhang, X.; Zhao, X.; Zhu, H.-L. Pyrazole Derivatives as Antitumor, Anti-Inflammatory and Antibacterial Agents. *Mini-Rev. Med. Chem.* **2013**, *13*, 1957−1966.

(8) Liu, X. R.; Wu, H.; He, Z. Y.; Ma, Z. Q.; Feng, J. T.; Zhang, X. Design, Synthesis and Fungicidal Activities of Some Novel Pyrazole Derivatives. *Molecules* **2014**, *19*, 14036−14051.

(9) Mor, S.; Khatri, M.; punia, R.; Sindhu, S. Recent Progress in Anticancer Agents Incorporating Pyrazole Scaffold. *Mini-Rev. Med. Chem.* **2022**, *22*, 115−163.

(10) Cuartas, V.; Robledo, S. M.; Vélez, I. D.; Crespo, M. D. P.; Sortino, M.; Zacchino, S.; Nogueras, M.; Cobo, J.; Upegui, Y.; Pineda, T.; Yepes, L.; Insuasty, B. New Thiazolyl-Pyrazoline Derivatives Bearing Nitrogen Mustard as Potential Antimicrobial and Anti-protozoal Agents. *Arch. Pharm.* **2020**, *353*, No. e1900351.

(11) Kumar, G.; Siva Krishna, V.; Sriram, D.; Jachak, S. M. Pyrazole-Coumarin and Pyrazole-Quinoline Chalcones as Potential Anti-tubercular Agents. *Arch. Pharm.* **2020**, *353*, No. 2000077.

(12) Ismail, A. H.; Abdula, A. M.; Tomi, I. H.; Al-Daraji, A. H.; Baqi, Y. Synthesis, Antimicrobial Evaluation and Docking Study of Novel 3,5-Disubstituted-2-Isoxazoline and 1,3,5-Trisubstituted-2-Pyrazoline Derivatives. *Med. Chem.* **2021**, *17*, 462−473.

(13) Matiadis, D.; Sagnou, M. Pyrazoline Hybrids as Promising Anticancer Agents: An up-to-Date Overview. *Int. J. Mol. Sci.* **2020**, *21*, 1−41.

(14) Desai, N. C.; Vaja, D. V.; Monapara, J. D.; Manga, V.; Vani, T. Synthesis, Biological Evaluation, and Molecular Docking Studies of Novel Pyrazole, Pyrazoline-Clubbed Pyridine as Potential Antimicro-bial Agents. *J. Heterocycl. Chem.* **2021**, *58*, 737−750.

(15) Zala, M. J.; Vora, J. J.; Khedkar, V. M. Synthesis and Molecular Docking Study of Arylsulfanyl Pyrazolylpyrazoline Derivatives as Antitubercular Agents. *Russ. J. Org. Chem.* **2021**, *57*, 2054−2062.

(16) Zala, M. J.; Vora, J. J. One-Pot Multicomponent Synthesis and Characterization of Some New Pyrazolylpyrazoline Scaffolds as Antitubercular and Antimalarial Agents. *Russ. J. Org. Chem.* **2021**, *57*, 1725−1732.

(17) Amir, M.; Kumar, H.; Khan, S. A. Synthesis and Pharmacological Evaluation of Pyrazoline Derivatives as New Anti-Inflammatory and Analgesic Agents. *Bioorg. Med. Chem. Lett.* **2008**, *18*, 918−922.

(18) Liao, L.; Jiang, C.; Chen, J.; Shi, J.; Li, X.; Wang, Y.; Wen, J.; Zhou, S.; Liang, J.; Lao, Y.; Zhang, J. Synthesis and Biological Evaluation of 1,2,4-Triazole Derivatives as Potential Neuroprotectant against Ischemic Brain Injury. *Eur. J. Med. Chem.* **2020**, *190*, No. 112114.

(19) Pokuri, S.; Singla, R.; Bhat, V.; Shenoy, G. Insights on the Antioxidant Potential of 1, 2, 4-Triazoles: Synthesis, Screening & QSAR Studies. *Curr. Drug Metab.* **2014**, *15*, 389−397.

(20) Chu, X. M.; Wang, C.; Wang, W. L.; Liang, L. L.; Liu, W.; Gong, K. K.; Sun, K. L. Triazole Derivatives and Their Antiplasmodial and Antimalarial Activities. *Eur. J. Med. Chem.* **2019**, *166*, 206−223.

(21) El-Saghier, A. M.; Mohamed, M. A.; Abd-Allah, O. A.; Kadry, A. M.; Ibrahim, T. M.; Bekhit, A. A. Green Synthesis, Antileishmanial Activity Evaluation, and in Silico Studies of New Amino Acid-Coupled 1,2,4-Triazoles. *Med. Chem. Res.* **2019**, *28*, 169−181.

(22) Bekircan, O.; Menteşe, E.; Ülker, S.; Kucuk, C. Synthesis of Some New 1,2,4-Triazole Derivatives Starting from 3-(4-Chlor-ophenyl)-5-(4-Methoxybenzyl)-4H-1,2,4-Triazol with Anti-Lipase and Anti-Urease Activities. *Arch. Pharm.* **2014**, *347*, 387−397.

(23) Kaproń, B.; Czarnomysy, R.; Wysokiński, M.; Andrys, R.; Musilek, K.; Angeli, A.; Supuran, C. T.; Plech, T. 1,2,4-Triazole-Based Anticonvulsant Agents with Additional ROS Scavenging Activity Are Effective in a Model of Pharmacoresistant Epilepsy. *J. Enzyme Inhib. Med. Chem.* **2020**, *35*, 993−1002.

(24) Cao, X.; Wang, W.; Wang, S.; Bao, L. Asymmetric Synthesis of Novel Triazole Derivatives and Their in Vitro Antiviral Activity and Mechanism of Action. *Eur. J. Med. Chem.* **2017**, *139*, 718−725.

(25) Dhiman, N.; Kaur, K.; Jaitak, V. Tetrazoles as Anticancer Agents: A Review on Synthetic Strategies, Mechanism of Action and SAR Studies. *Bioorg. Med. Chem.* **2020**, *28*, No. 115599.

(26) Li, Y. T.; Yao, W. Q.; Zhou, S.; Xu, J. X.; Lu, H.; Lin, J.; Hu, X. Y.; Zhang, S. K. Synthesis, Fungicidal Activity, and 3D-QSAR of Tetrazole Derivatives Containing Phenyloxadiazole Moieties. *Bioorg. Med. Chem. Lett.* **2021**, *34*, No. 127762.

(27) Gao, C.; Chang, L.; Xu, Z.; Yan, X. F.; Ding, C.; Zhao, F.; Wu, X.; Feng, L. S. Recent Advances of Tetrazole Derivatives as Potential Anti-Tubercular and Anti-Malarial Agents. *Eur. J. Med. Chem.* **2019**, *163*, 404−412.

(28) Desai, N. C.; Trivedi, A.; Somani, H.; Jadeja, K. A.; Vaja, D.; Nawale, L.; Khedkar, V. M.; Sarkar, D. Synthesis, Biological Evaluation, and Molecular Docking Study of Pyridine Clubbed 1,3,4-Oxadiazoles as Potential Antituberculars *Synth. Commun.* 2018, 485 524 540 DOI: 10.1080/00397911.2017.1410892.

(29) Naveen, G.; Peerapur, B. V. Comparison of the Lowenstein-Jensen Medium, the Middlebrook 7H10 Medium and MB/BACT for the Isolation of *Mycobacterium Tuberculosis* (MTB) from Clinical Specimens. *J. Clin. Diagn. Res.* **2012**, *6*, 1704−1709.

(30) Friesner, R. A.; Banks, J. L.; Murphy, R. B.; Halgren, T. A.; Klicic, J. J.; Mainz, D. T.; Repasky, M. P.; Knoll, E. H.; Shelley, M.; Perry, J. K.; Shaw, D. E.; Francis, P.; Shenkin, P. S. Glide: A New Approach for Rapid, Accurate Docking and Scoring. 1. Method and Assessment of Docking Accuracy. *J. Med. Chem.* **2004**, *47*, 1739−1749.

(31) Holas, O.; Ondrejcek, P.; Dolezal, M. *Mycobacterium Tuberculosis* Enoyl-Acyl Carrier Protein Reductase Inhibitors as Potential Antituberculotics: Development in the Past Decade. *J. Enzyme Inhib. Med. Chem.* **2015**, *30*, 629−648.